THE EFFECT OF FORGING TEMPERATURE ON CARBIDE PRECIPITATION AND DUCTILITY OF HAYNES 230 NICKEL-BASED SUPERALLOY

By: Thomas Chludzinski
Advisor: Dr. Blair London
Industry Sponsor: Carlton Forge Works

Approval Page

Project Title: Effects of Forging Temperature on Carbide Precipitation and Ductility of Haynes 230 Ni-Based Superalloy

Author: Thomas Chludzinski

Date Submitted: June 1, 2012

CAL POLY STATE UNIVERSITY
Materials Engineering Department

Since this project is a result of a class assignment, it has been graded and accepted as fulfillment of the course requirements. Acceptance does not imply technical accuracy or reliability. Any use of the information in this report, including numerical data, is done at the risk of the user. These risks may include catastrophic failure of the device or infringement of patent or copyright laws. The students, faculty, and staff of Cal Poly State University, San Luis Obispo cannot be held liable for any misuse of the project.

Prof. Blair London
Faculty Advisor

_____
Signature

Prof. Trevor Harding
Department Chair

_____
Signature

1 Abstract

Samples of Haynes 230 nickel-based superalloy were taken from forgings at Carlton Forge Works. These samples represented components that passed and failed ductility specification. Metallographic measurements of particle size and intergranular particle count were taken from 25 locations across the sample. Carbide particles at the grain boundaries were equal size, averaging 13.0 μm in diameter. The low ductility samples contained an average of twelve particles per 250 μm of grain boundary, high ductility samples contained an average of only four particles along the same grain boundary length. To determine the effects of forging temperature on carbide distribution in the microstructure, three 4-in-diameter, 4-in-height Haynes 230 billets were upset forged to 7-in-diameter, 1-in-height at 2050°F, 2150°F, and 2250°F. For each forging, samples were removed and solutionized at 2150°F, 2200°F, and 2250°F for 45 minutes. Each combination of forging temperature and solutionizing temperature was tensile tested to determine yield strength and ductility. Results showed the alloy increased ductility with forging temperature, which corresponded to decreased particle count. Mechanical properties were altered less prominently with solutionizing temperature, but a small increase in tensile strength and decrease in ductility was associated with higher temperature solutionizing, accompanied by a decreased particle size. Particle count and distribution were found to the key factor in determining ductility of the material. Forging at low temperatures causes plastic deformation at the grain boundaries, providing a low energy nucleation site for migrating carbon in solution, thereby increasing the number of particles in the forged pieces. The optimal combination of ductility and yield strength occurred at 2150°F forging temperature and 2200°F solutionizing temperature.

Keywords: Materials Engineering, Forging, Haynes 230, Superalloy, Carbide, Precipitation, Ductility

Table of Contents

2 List of Figures

3 List of Tables

4 Introduction

4.1 Purpose

Carlton Forge Works (CFW) has experienced quality assurance issues with rings forged from Haynes 230 Ni-based superalloy. Samples of the finished components undergo mechanical testing for yield strength, ultimate tensile strength, and ductility to assure compliance with specified performance requirements. The most common parameter failed is the ductility specification. Samples of Haynes 230 are occasionally tested to have much lower maximum elongation than is required. This issue is believed by CFW to be attributed to the size and distribution of carbide phases within the material. The purpose of this project is to determine the cause of the low ductility and offer a solution.

4.2 Carlton Forge Works

CFW is a forging company based out of Paramount, CA who produces forged components for the aerospace, gas turbine, industrial, and nuclear industries. Founded in 1929, CFW produces a variety of rings and open and closed forgings from such alloys as nickel, titanium, aluminum, cobalt, zirconium, niobium, and iron. They are capable of forging components up to 180 inches, and as small as 4 inches, with a hammer capacity of 12,000 pounds at the Paramount facility, although for closed die components and ingot and billet conversion, the capacity can be expanded to 50,000 pounds, at the forging facility in Oxnard, CA[1].

4.3 Haynes 230 Background

CFW forges gas turbine components, namely combustion chambers, from Haynes 230 nickel-based superalloy (Figure 1). Haynes 230 can resist oxidation for an extended period in temperatures up to 1149°C[2]. With operating temperatures in the range of 900°C, the high temperature oxidation resistance is important for component longevity[3,4]. Haynes 230 also features resistance to grain coarsening, allowing it to maintain its strength characteristics over extended periods of high temperature use. The ductility of Haynes 230 is responsible for its resistance of high cycle fatigue created by the pulsating combustion reaction[4].

Processing of Haynes 230 from bulk ingot form is a simple process. The ingots come in the solution treated state, in which the alloy is ductile and readily formed. The alloy can then be heated to forging temperature and shaped. Subsequent heat treatment and cooling methods are aimed to control the size and dispersion of carbide precipitates.

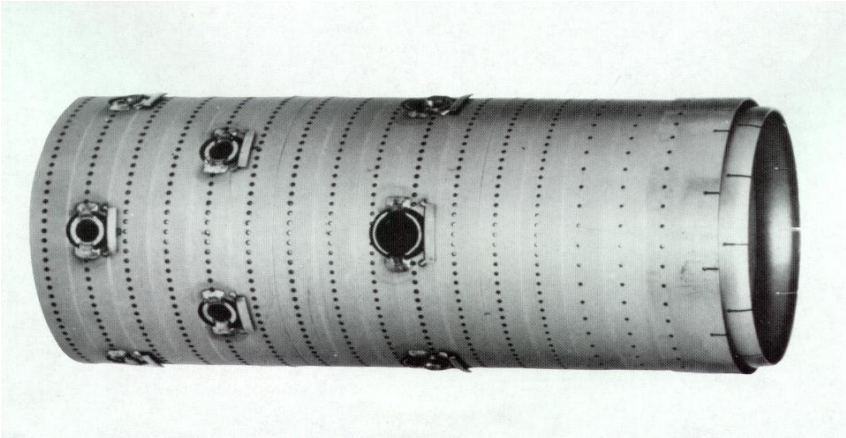

Figure 1: Haynes 230 combustor for a gas turbine engine[2].

4.4 The Gas Turbine Engine

The gas turbine engine is comprised of three major components: compressor, combustor, and turbine (Figure 2). The compressor is a relatively low temperature component that serves to compress incoming air, and has little need for a high temperature superalloy such as Haynes 230, but is instead made from titanium alloys. The areas of the engine that require high temperature superalloys are the combustor and the turbine. The combustor injects fuel into the compressed air and ignites the mixture. The hot gasses from the combustion flow into the turbine where work is extracted[3].

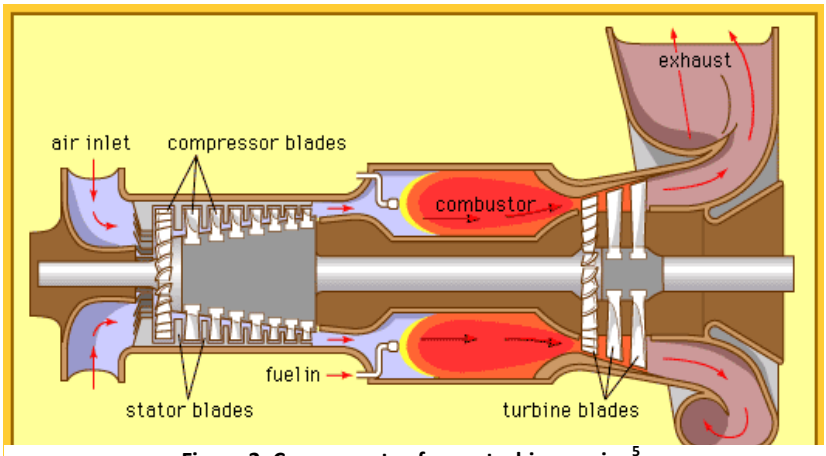

Figure 2: Components of a gas turbine engine[5].

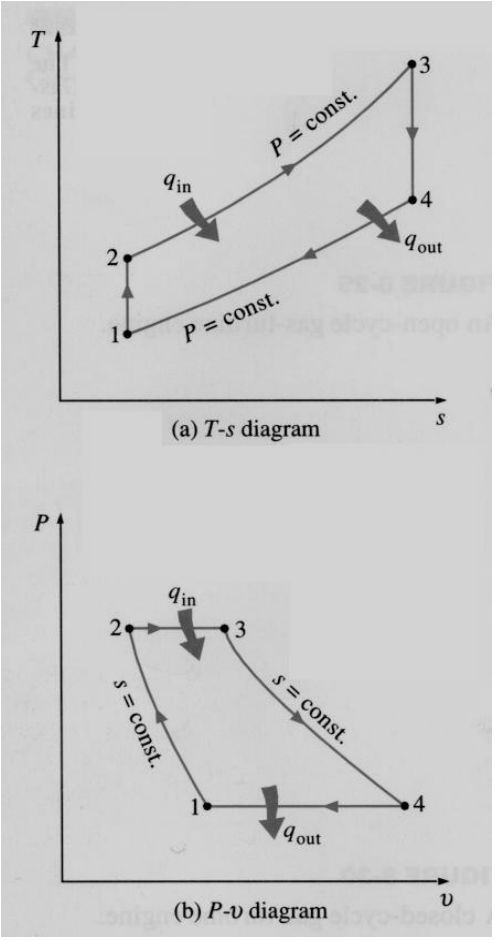

Figure 3: (a) T-s diagram and (b) P-v diagram of an ideal gas turbine engine[6].

Modern gas turbine engines attempt to model the Brayton cycle of an ideal gas. The steps of the cycle (Figure 3) are isentropic compression in the compressor, isobaric heating in the combustor, isentropic expansion in the turbine, and isobaric cooling which is replicated by the inputting air from outside the engine rather than cooling the exhaust gasses. Although the derivation is not discussed here, the ideal efficiency of this cycle may be predicted by equation 1[3] where η is the ideal efficiency, T_2 is the temperature of the cold reservoir or the temperature of the gas in the combustor, and T_1 is the temperature of the combusted gas (Figure 3).

$$\boldsymbol{\eta = 1 - \frac{T_2}{T_1}}$$

Equation 1: Efficiency of Brayton Cycle.

It follows then that by decreasing T_2 and increasing T_1, the efficiency of the engine increases. As such materials capable of operating in high temperature and high pressure environments are required to accommodate a higher T_1. Nickel-based superalloys are most frequently used in the fabrication of components such as the combustor and turbine as these areas are subjected to the highest temperatures and pressures in the engine. Turbine blades must operate with minimal creep in order to maintain a narrow clearance between the blades and the turbine casing. Creep of the blade would result in a collision between the blade and the wall, causing catastrophic engine failure. For this reason blades are most often made from single crystal superalloys, which contain no grain boundaries thus eliminating grain boundary sliding.

The combustor does not require as high of creep resistance as the turbine blades. The function of the combustor is to contain and direct combusting gasses into the turbine, and must therefore be capable of maintaining high strength at combustion temperature. Ductility of the alloy used in the combustor must

be higher than that used in the turbine blades, as ductile failure is the desired mode of rupture in the combustor to minimize the risk for catastrophic failure[3].

4.5 Forging

Forging of components for engine use occurs predominantly through open forging methods. Combustor rings are forged by ring rolling for the desired inner and outer diameter (Figure 4). Sections of material are removed from a billet and heated to forging temperature, for Haynes 230, the recommended forging temperature is 2150°F. The workpiece is then punched through the center to insert the inner diameter roller. An outer diameter roller is applied to the surface, and the workpiece is rotated between the two rollers as the distance between the rollers is reduced until the ring has the appropriate inner and outer diameter[7].

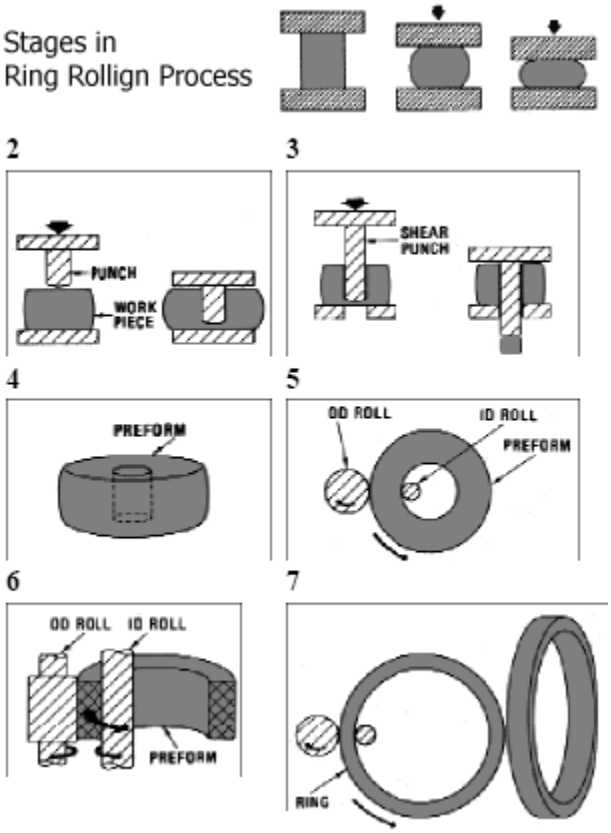

Figure 4: Steps of ring rolling[7].

4.6 Nickel-Based Superalloys

Nickel-based superalloys were developed in the 1950s for use in high temperature applications due to their unique ability to maintain high strength at high temperatures often exceeding 0.8 T_m. Another important aspect of superalloys is their ability to resist corrosion and creep at high temperatures. Many superalloys form a stable passivating layer at high temperatures protecting the alloy from oxidation. Creep resistance of the superalloys depends strongly on the composition and processing of the alloy, and can be attributed to such characteristics as the stability of the austenitic matrix, yield stress anomaly, grain size, and presence of carbides[8,9,10].

4.6.1 Composition

The first and most apparent method to control the properties of any alloy is to control the type and amount of elements within. In the case of Ni-based superalloys, there are three classes of elements added in varying weight percentages, depending on the application and processing of the alloy. The first class of elements act to form and stabilize the primary ϒ phase. These include nickel, cobalt, iron, chromium, ruthenium, molybdenum, rhenium, and tungsten, with nickel being the majority element in any nickel-based superalloy. Nickel exhibits a Face Centered Cubic (FCC) crystal structure and elements in this first class are of similar in atomic radius and electron configuration, and therefore are used to provide the benefits of solid solution strengthening in the FCC ϒ phase.

The second class of elements present in Ni-based superalloys are used to promote the precipitation of the ordered ϒ' phase. This group contains such elements as aluminum, titanium, niobium, and tantalum. These elements are of a larger atomic radius than nickel, and with an electron configuration that favors ordering with nickel over solid solution. The compounds formed usually follow the structure of Ni_3(Al, Ti, Nb, Ta) although other formations are possible such as that found in the ϒ'' phase.

The third class of elements that are added to the superalloys are used to form grain boundary stabilizing phases. These elements are carbon, boron, and zirconium. These alloying elements represent the minority elements of the alloy system. They react with many of the elements present in the alloy to form ordered compounds that most often appear at the grain boundaries, although can present themselves in many areas throughout the alloy.

The relative amounts of these alloying elements vary widely based on the expected operating conditions of the alloy. Single crystal superalloy turbine blades, for instance, have little need for grain boundary stabilizers considering the lack of grain boundaries. For applications that require the high tensile strength at high homologous temperatures, a high volume fraction of Υ' is favorable, and therefore a larger presence of group two alloying elements will be observed.

Haynes 230 is used primarily in applications where a high ductility is given a higher priority than high strength at elevated temperatures. As such it is observed that the prominent strengthening mechanism is solid solution strengthening. Haynes 230 has a relatively large presence of tungsten and chromium to facilitate this strengthening (Table I). Group three elements also play an important role in the ductility and creep resistance, and therefore carbon is added in relatively large quantities[3,4,8].

Table I: Chemical Composition of Haynes 230 in Weight %[2]

Ni	Cr	W	Mo	Fe	Co	Mn	Si	Al	C	La	B
57	22	14	2	3	5	0.5	0.4	0.3	0.1	0.02	0.015

4.6.2 Phases and Microstructure

As indicated by the previous section, there are three dominant phases present in Ni-based Superalloys. The most prominent phase representing the largest volume fraction of the material is the austenitic Υ phase. This phase is FCC in structure and always contains some amount of alloying element to strengthen and stabilize it. This phase is the matrix phase in which all subsequent phases precipitate (Figure 5). Nickel exhibits and nearly filled third electronic shell which allows it to interact with the group one elements (see previous section) without losing phase stability[4].

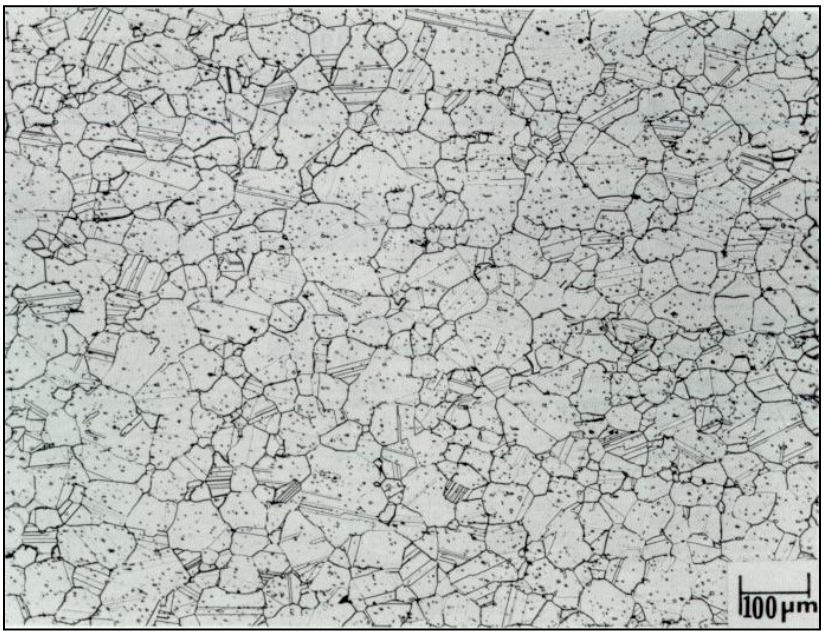

Figure 5: Hayes 230 typical microstructure. The austenitic gamma phase comprises the matrix, with carbides and twinning planes also clearly visible[2].

Superalloys in general gain most of their high temperature strength from the presence of the ordered Υ' phase. This phase has the chemical composition of $Ni_3(Al, Ti, Nb, Ta)$. The Υ' phase orders in a primitive cubic, $L1_2$ structure which is similar to the FCC Υ phase, with a slightly different lattice parameter (Figure 6). The combination of similar structure and similar lattice parameter to the austenitic phase allows for an even precipitation of the Υ' particles, and allows them to remain coherent in the matrix at relatively large sizes. It is due to this coherence that the Υ' phase in not visible in Figure 1. The presence of Υ' is vital for the yielding behavior of these alloys. As temperature increases, the yield strength of superalloys increases to a point (Figure 7). This is attributed mismatch between stoichiometric ratio the Υ' compound and the ratio of Ni:(Al, Ti, Nb, Ta) required to form a perfect $L1_2$ crystal structure, although this mechanism is controversial and not fully understood. Simply put, Anomalous Yielding Effect is the dissolution of migrating defects in the Υ' phase. When a dislocation reaches the boundary of the coherent precipitate, the dislocation is incorporated into the particle leaving the surrounding Υ dislocation free. As temperature increases, the increase in mobility of these dislocations allows for faster dissolution of dislocations, thus increasing the yield strength of the alloy. This effect is overcome around 800°C when the stability of the Υ' particle becomes low enough to begin solutionizing[3].

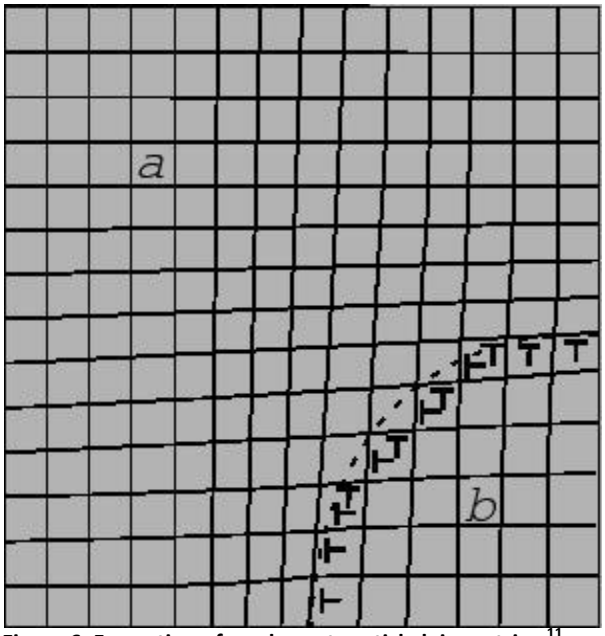

Figure 6: Formation of a coherent particle b in matrix a[11].

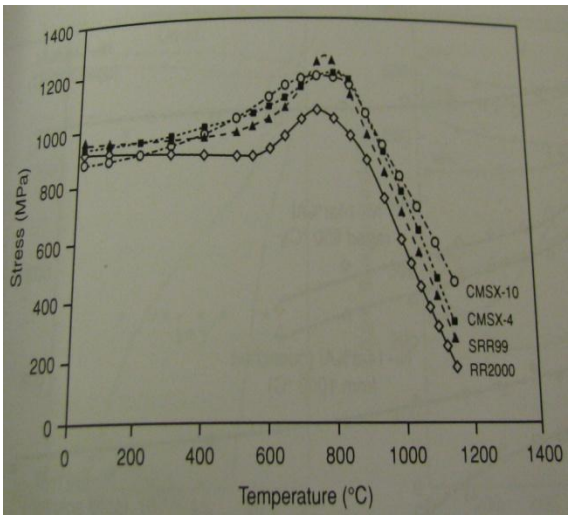

Figure 7: Demonstration of Anomalous Yielding Effect of various superalloys. Note this increase in rupture stress with temperature up until roughly 800°C[3].

The third phase present in superalloys, and the most important phase to this project is carbides. Carbides precipitation can be controlled to tailor the mechanical properties of a forged superalloy. Primary carbides follow a 1:1 stoichiometric ratio with its complimentary metal, MC, where M can be virtually any of the alloying elements, although the strongest carbide formers are chromium, tungsten, molybdenum, titanium, tantalum, and hafnium. Primary carbides precipitate at high temperatures from the liquid, although not all carbon in the liquid will form carbides. Much of the carbon will remain in solution in the austenitic ϒ phase. The carbides within the ϒ matrix are often these MC carbides (Figure 4). Secondary carbides are those with a more complicated stoichiometric ratio such as $M_{23}C_6$. These carbides are formed by decomposition of the primary carbides, as well as through precipitation from the ϒ matrix at approximately 750°C. These carbides tend to form at the ϒ-ϒ grain boundaries, as the grain boundary region contains the highest concentration of carbon[3,8].

4.6.3 Effects and Control of Carbide Precipitation

The size and morphology of carbides play an important role in their effect on mechanical behavior. Secondary carbides tend to form along the grain boundaries of wrought superalloys. As such, they can act to stabilize the grain boundaries to reduce creep and improve ductility[3,8]. Ductility of the alloy is improved with finely dispersed small carbides along the grain boundary, such that particle size is less than or equal to 5-7 μm[12,13]. Large precipitates act to reduce ductility as they interfere with dislocation movement[14].

Controlling the formation of these carbides is essential to control the mechanical properties of the alloy. Carbide dispersion is controlled through the level of supersaturation of carbon within the system, as well as through hot working. In an alloy system that favors a fine dispersion of carbides, the first method of control is to introduce and control dislocation density of the alloy. This can be done by controlling the temperature of forging along with degree of deformation. High temperature forgings reduce dislocation density of the forged component, thereby reducing the number of nucleation sites for the carbides. Lowering the nucleation sites directly increases the size of the particles precipitated. A high degree of deformation and working can act to homogenize the dislocations, which corresponds to an even dispersion of dislocations and carbides. It is also common practice to solution treat a component to bring some of the secondary carbides into solution followed by quenching to supersaturate the component. This serves to reduce the size of carbide particles at the grain boundaries.

4.7 Realistic Constraints[14]

The information yielded in this project may potentially be applied to the ring rolling process at CFW for turbine components forged of Haynes 230. As such, this research has effects beyond the improvement of forging conditions. To determine the broader impacts of this research, the application of these components and the stakeholders of these components must also be considered.

4.7.1 Economic Impact

Components forged of Haynes 230 are subjected to an energy intensive production process representing a large investment in addition to the high material cost of the superalloy. Any component that fails material property specifications is given another energy intensive treatment and retested. This is repeated a second time if the component fails again, but is discarded upon failure after the third treatment due to gamma prime particle coarsening[15]. Components that have failed ductility specifications are sold to a recycling plant for a fraction of the cost invested into them. These occurrences, however infrequent, cause considerable time and monetary loss to CFW. Lowering the incidence of component failure will result in the lower product waste allowing for higher net profit and a more competitive manufacturing operation.

4.7.2 Health and Safety Impact

Jet engine combustors have a specific set of requirements for safe operations. Two of these requirements are a specific minimum ductility specification and a minimum yield strength. Ductility

requirements are necessary to ensure ductile fracture in the event of a combustor failure[16]. This failure mode is characterized by slow crack propagation, which is desired in a combustor. If a combustor were to fail by brittle fracture, as might be the case with a combustor that did not pass ductility specifications, the failure would result in immediate loss of engine pressure and burn out the combustion. A ductile failure will fail overtime, gradually reducing engine pressure giving the pilot a better chance of conducting a safe emergency landing. Yield strength requirements are in place to match and exceed the maximum pressures to which the component will be exposed. Decreasing the percentage of failed components reduces the risk of installing an unsafe component, making for safer air travel.

5 Experimental Procedure

5.1 Metallography

Material samples of Haynes 230 in various forged conditions were provided by CFW including samples of as-cast Haynes 230 starting material, samples that failed ductility specification, and samples that passed ductility specification (Table II). Samples were mounted in mineral filled Diallyl-Phthalate (Bakelite) and polished by standard methods up to 3 µm finish. Polished samples were then etched in a solution containing approximately 95% HCl, 5% H_2O_2, submerged for a period of thirty seconds to one minute. Measurements of carbide size and distribution were measured with an Olympus BX41M optical microscope and ImagePro Express 6.0 software. Images were taken at 500x magnification with a grain boundary crossing through the vertical view field. Particles were counted along that boundary, and diameters of three particles were measured (Figure 8). This process was repeated at 25 locations for each sample.

Table II: Mechanical Properties of Provided Samples

Condition	Yield Strength (ksi)	UTS (ksi)	Ductility (%)
Requirement	45	110	40
As Cast	51	124	48.2
Passed Inspection	66.5	126	51
Failed Inspection	52	98	24

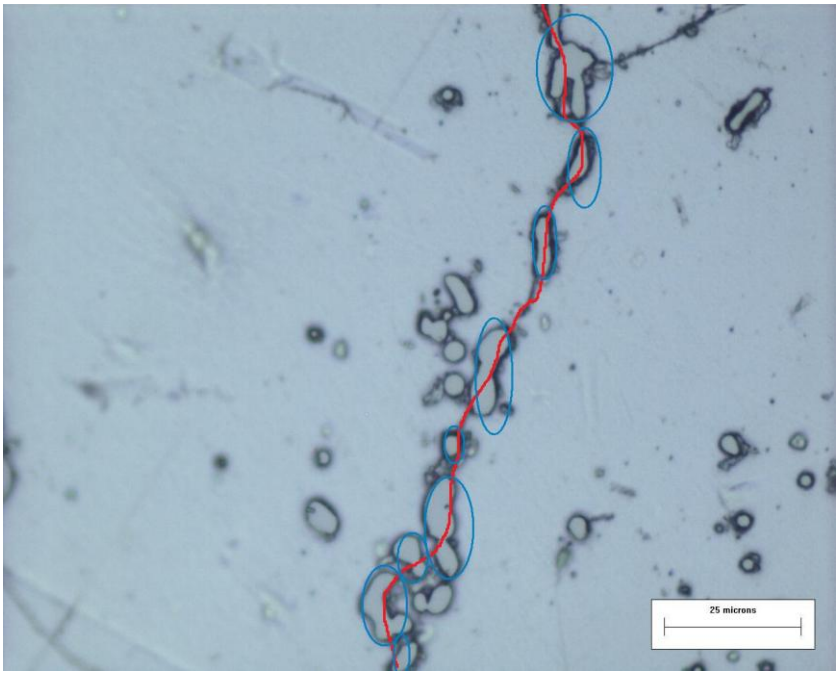

Figure 8: Sample measurement from the failed Haynes 230 Sample. Red indicates the grain boundary being observed, blue circles enumerate carbides present.

5.2 Forging Experiment

An experiment was conducted at CFW to test the effects of forging temperature and solutionizing temperature on the size and distribution of carbides within the forged specimen (Table III). Three sections of a 4 inch diameter billet were cut to be four inches in length each (Figure 9), and designated sections A, B, and C. Each piece was heated for 30 minutes to their respective forging temperatures of either 2050°F, 2150°F, or 2250°F. The hot workpieces were then upset forged to a thickness of 1 inch from repeated hammer pressing, and fan cooled. Each section was the cut via water jet at Creative Cutting in San Luis Obispo, California to remove six rectangular bars along the radius (Figure 10). These six bars per section were divided into two groups of three bars per section, and these groups subjected to one of two solutionizing temperatures of either 2100°F, or 2200°F for 45 minutes per group.

Table III: Forging Experiment Methodology

	Section A		**Section B**		**Section C**	
Forge Temp (F)	2050		2150		2250	
Cutting Group	**1**	**2**	**1**	**2**	**1**	**2**
Solution Temp (F)	2100	2200	2100	2200	2100	2200

Figure 6: Starting as-cast Haynes 230 section, 4 inches in diameter and 4 inches in height for forging experiment.

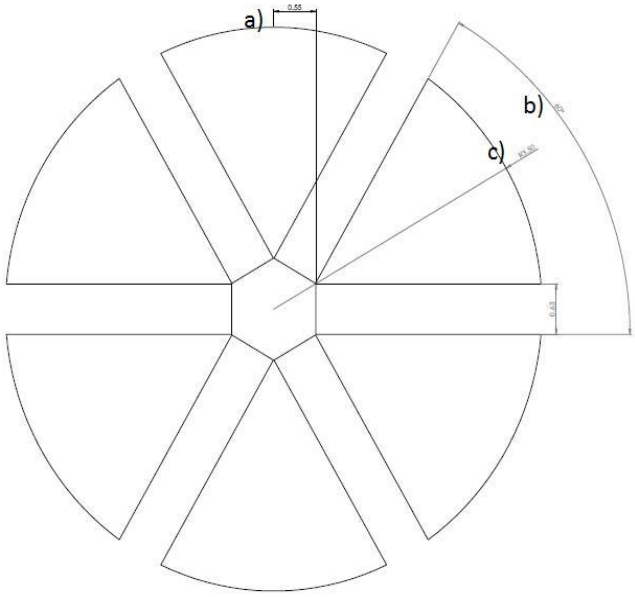

Figure 10: Cutting plan to remove bars from forges sections. a) distance from the center is equal to 0.55 inches, b) angular offset of each sample is 60°, c) sample radius of 3.5 inches. The rectangular sections between the wedges are the bars which are removed for solutionizing and mechanical testing.

Samples were arranged by forging and solutionizing temperatures into groups A1, A2, B1, B2, C1, and C2. Metallographic measurements were made of each forging/solutionizing combination, using the same procedure as in the previously described section. The bars were sent to a machine shop to be cut into round tensile bars. In total, six forging/solutionizing combinations were observed with three samples per combination.

5.3 Mechanical Properties Testing

After solutionizing, the samples were sent to a machine shop for turning and threading (Table IV). Machined samples were then used as round tensile bars. Each tensile bar was subjected to mechanical loading to determine the ductility, ultimate tensile strength and yield strength of the forging. This was conducted in an Instron tensile testing system, model 3369, with 9/16 x 12 threaded end.

Table IV: Tensile Bar Dimensions

Gauge Length	Diameter	Thread	Thread Length
1.45 inch	.252 inch	9/16 – 12	.75 inch

Tensile bars were threaded into an adapter, which allows for round tensile bars to be inserted into wedge grips. An extensometer of 1 inch gauge length was attached to the reduced section of the tensile samples. Samples were tested within the parameters of ASTM-E08, with an initial strain rate of 0.1 inch/minute. At an extension of 2%, the extensometer was removed, and straining was resumed at a rate of 0.5 inch/minute until the tensile bar fractured.

6 Results

6.1 Metallography

Metallographic data was collected via optical microstructure after imaging all six forging/solutionizing temperature combinations and the reference samples of passed and failed Haynes 230 forged components (Figures 11 – 18). A summary of average particle size and count is listed in Table V, with data taken from 25 locations per sample. First noted is the difference between passed and failed microstructures. Particle size appears nearly identical, but with a 300% increase in particle count from passed to failed microstructures.

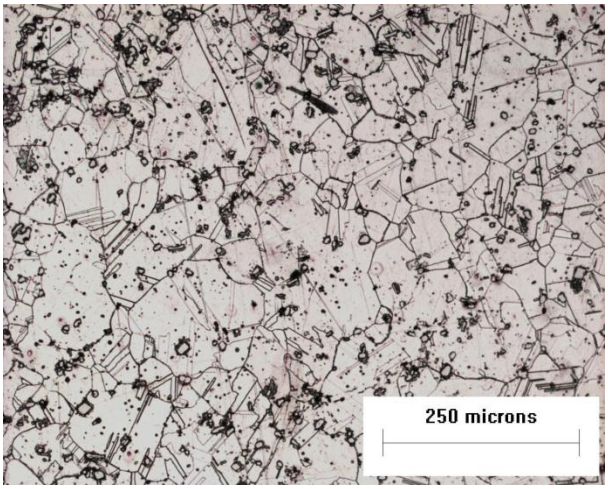

Figure 7: Reference sample of passed Haynes 230 at 200x magnification, etched in HCl and H_2O_2

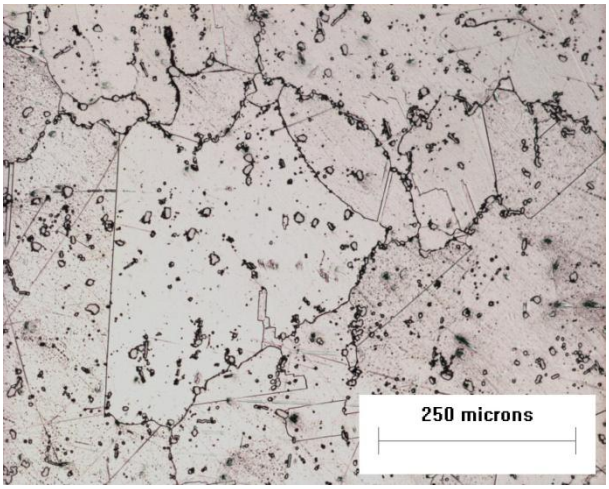

Figure 12: Reference sample of failed Haynes 230 at 200x magnification, etched in HCl and H_2O_2

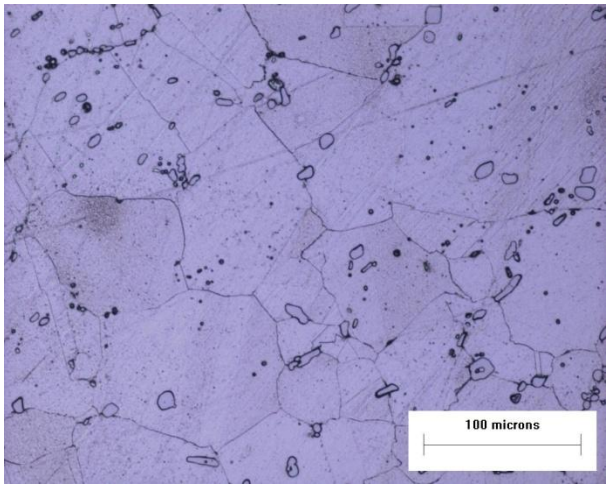

Figure 13: A1 sample at 200x magnification, etched in HCl and H_2O_2

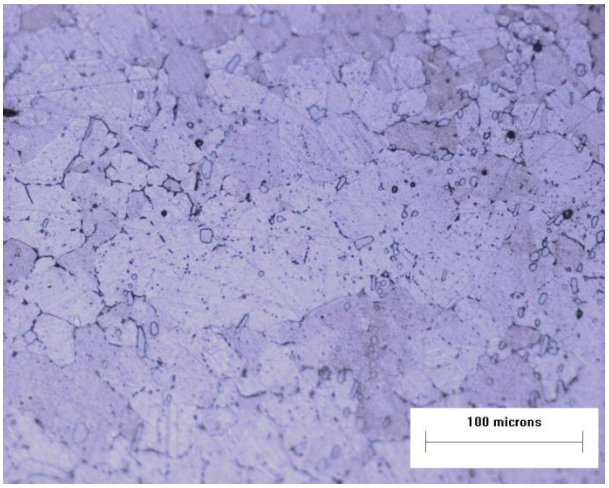

Figure 14: A2 sample at 200x magnification, etched in HCl and H_2O_2

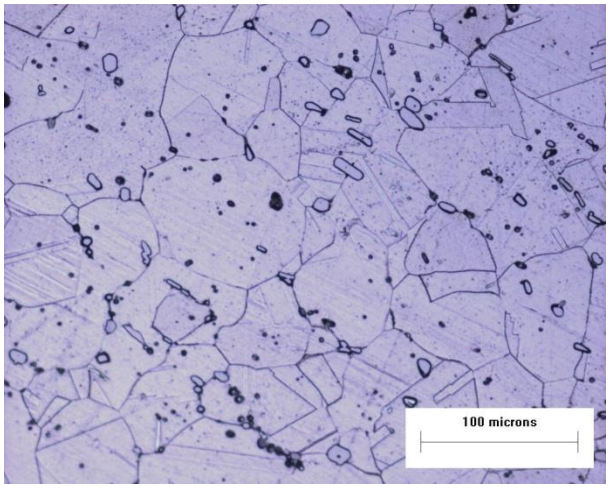

Figure 15: B1 sample at 200x magnification, etched in HCl and H_2O_2

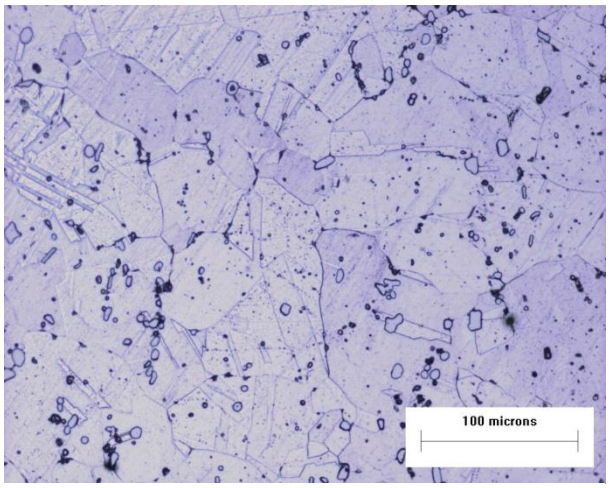

Figure 16: B2 sample at 200x magnification, etched in HCl and H_2O_2

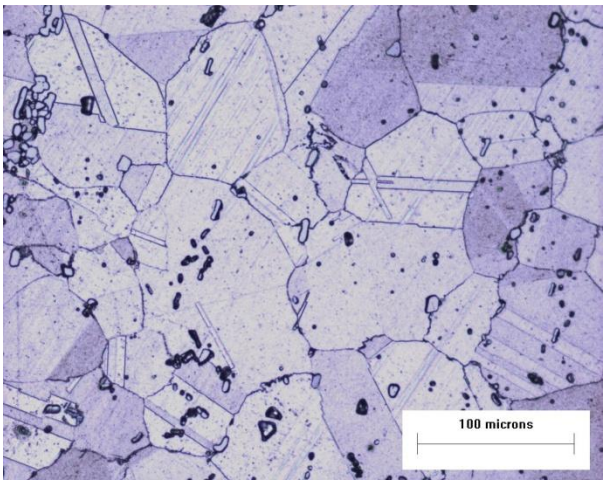

Figure 17: C1 sample at 200x magnification, etched in HCl and H_2O_2

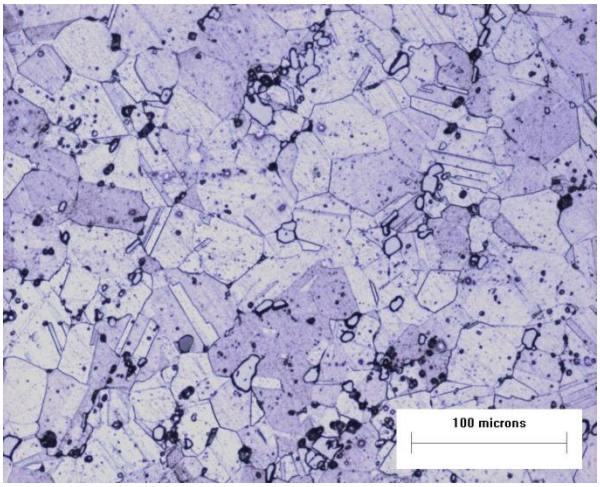

Figure 18: C2 sample at 200x magnification, etched in HCl and H_2O_2

Table V: Particle Size and Number of Particles on Grain Boundary for Haynes 230 Samples

Sample	Average Size (µm)	Average Count
Failed Ductility	13.2	12
Passed Ductility	12.8	4
Forge Sample A1	7.7	4
Forge Sample B1	8.5	6
Forge Sample C1	6.6	9
Forge Sample A2	1.6	19
Forge Sample B2	6.0	8
Forge Sample C2	6.7	10

Two-sample t-testing was used to assess the statistical similarity of particle size and count between the microstructures of the samples passing and failing ductility specifications provided by CFW. This analysis indicates no difference in particle size between the two samples (95% confidence, p = 0.23, Figure 19).

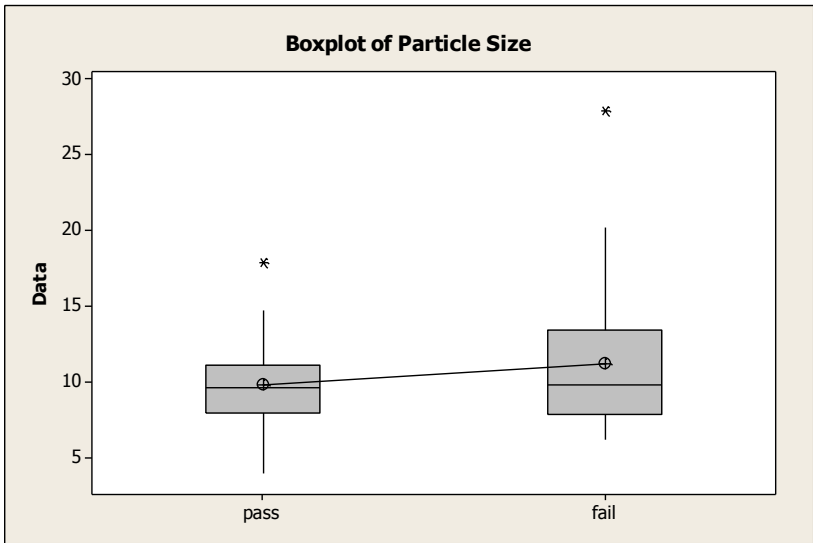

Figure 19: Boxplot of particle size data from passed and failed ductility samples indicating no statistically significant difference between the two.

Although the particle size between the samples are similar, the sample which failed ductility specifications contained an average of 300% higher particle count along the grain boundaries than the material which passed inspection, indicating an obvious difference in particle count between the samples. A Two-sample t-test was again used to confirm this finding (95% confidence, p = 0.000, Figure 20).

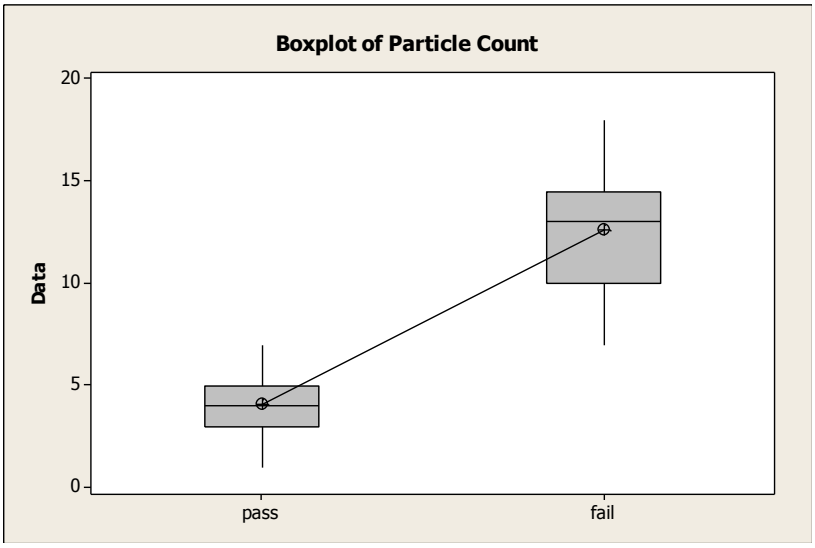

Figure 20: Boxplot of particle count data from passed and failed samples indicating a statistically significant difference between the two.

To determine to similarity of samples from the forging experiment to those which passed and failed ductility specifications, one-way ANOVA was used to compare particle size and count between the six forging/solutionizing temperature combinations and the passed and failed baseline samples (Figures 21, 22).

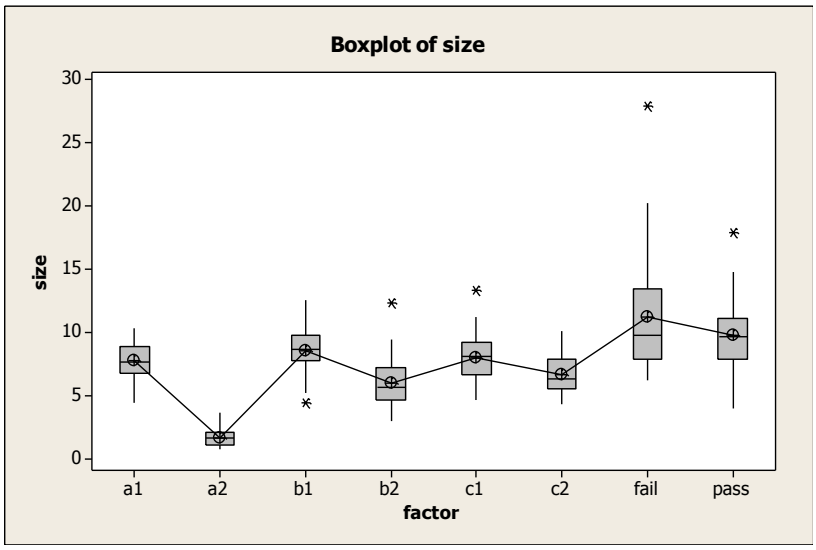

Figure 21: ANOVA test of particle size between samples, shows each forging condition produces similar size particles, with the exception of A2.

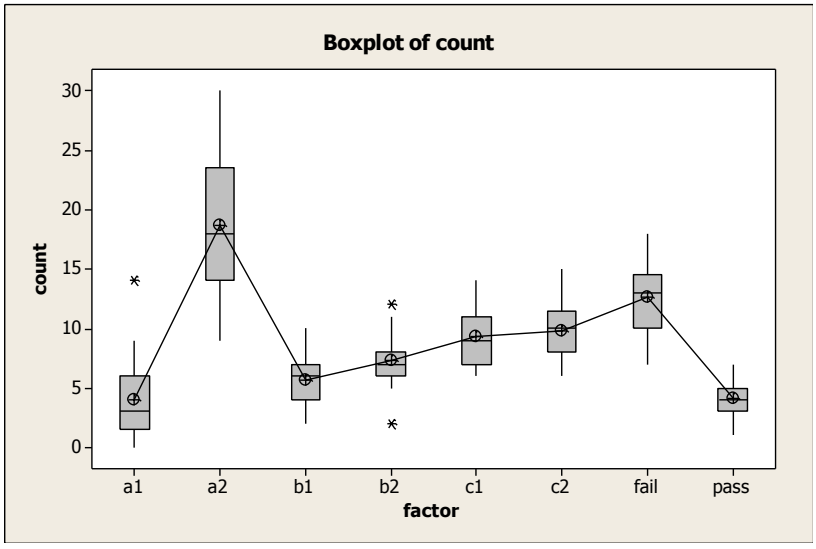

Figure 22: ANOVA test for particle count between samples, shows dependence of particle count along a grain boundary and forging temperature.

In each ANOVA test, the result showed the samples to be likely dissimilar (p = 0.000), as expected, meaning that neither particle size, nor particle count were constant for all samples. Samples A1, B1, and C1 do not contain particles of a significantly different size than the passed ductility sample, and are significantly different from the failed ductility sample (Figure 21), indicating a microstructural resemblance to the material which passed ductility specification. Only samples A1 and B1, however, were shown to have a similar particle counts to that of the passing sample through Tukey intervals (Figure 22). We can see from these results, then, that samples A1 and B1 are statistically similar to the microstructure of material which passed ductility specifications.

6.2 Mechanical Properties

Due to machining limitations, only 6 of the 18 total samples were mechanically tested (Figure 23). It can be seen, however, that the forging and testing conditions affected the mechanical properties.

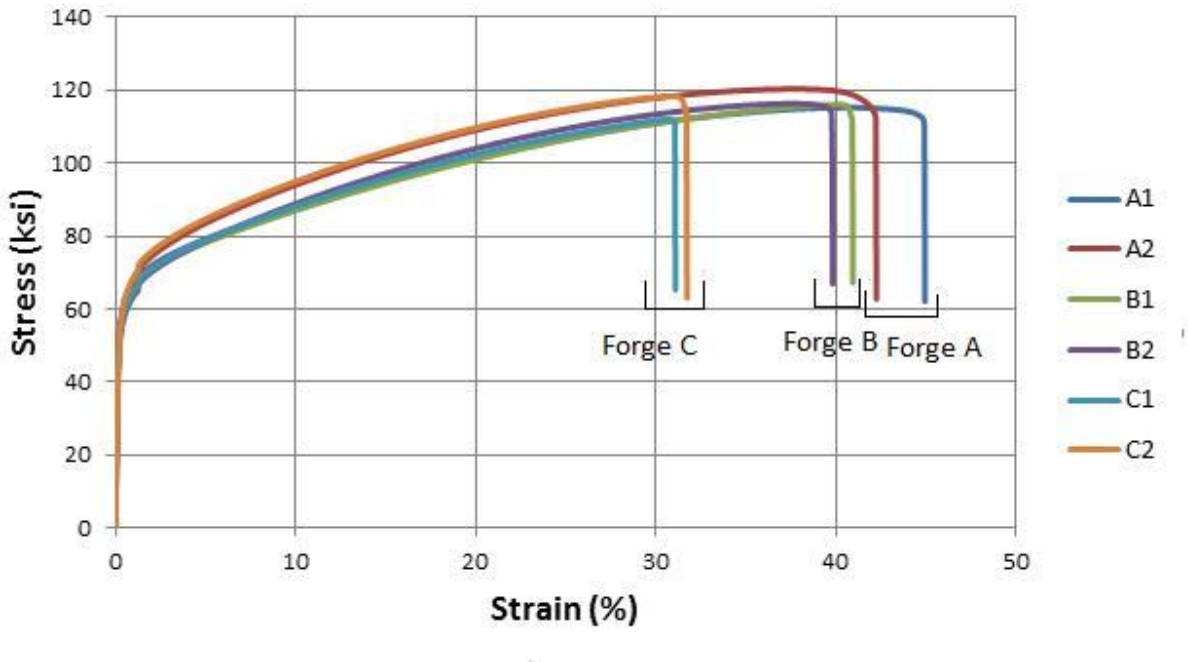

Figure 23: Stress and Strain Plot of all six forging/solutionizing combinations, note forging temperature A is the hottest, temperature C is the coldest, solutionizing temperature 1 is the hottest, and temperature 2 is the coldest.

The forging temperature has a strong correlation with ductility. Each sample of material forged at 2050°F failed before each sample forged at 2150°F, and that each sample forged at 2150°F failed before each sample forged at 2250°F. The relationship between solutionizing temperature and ductility is less

clear, however. There is not a consistent increase or decrease in ductility between the solutionizing temperatures of samples forged at the same temperature. The effect of solutionizing is pronounced in the analyzing the ultimate tensile strength of the samples, as can be seen in Table VI. Decreasing the solutionizing temperature of a sample increased the ultimate tensile strength of that sample.

Table VI: Tensile Properties of Forged Samples

Sample	Yield Strength (ksi)	Ultimate Tensile Strength (ksi)	Ductility (%)
Requirement	45.0	110.0	40.0
A1	59.06	115.22	44.89
A2	59.70	120.31	42.20
B1	57.47	116.03	40.89
B2	55.96	116.30	39.78
C1	57.50	111.98	31.04
C2	61.09	118.34	31.69

7 Discussion

The difference between the microstructures of samples that passed and failed ductility testing which can account for the change in properties lies with the carbides, as mentioned before. Notably, a clear increase in particle concentration can be seen in material that failed ductility specifications (Figure 19). Pairing this with the results of microstructural analysis of the forging temperature experiment, it is noted that a decrease in forging temperature results in a similar increase in particle concentration (Figure 22). This can be associated with the phenomenon of microcavitation occurring during forging process (Baldan, 1992). Microcavitation occurs during the forging, and can be seen a small voids at the grain boundaries, particularly in areas of high stress concentration (Figure 24).

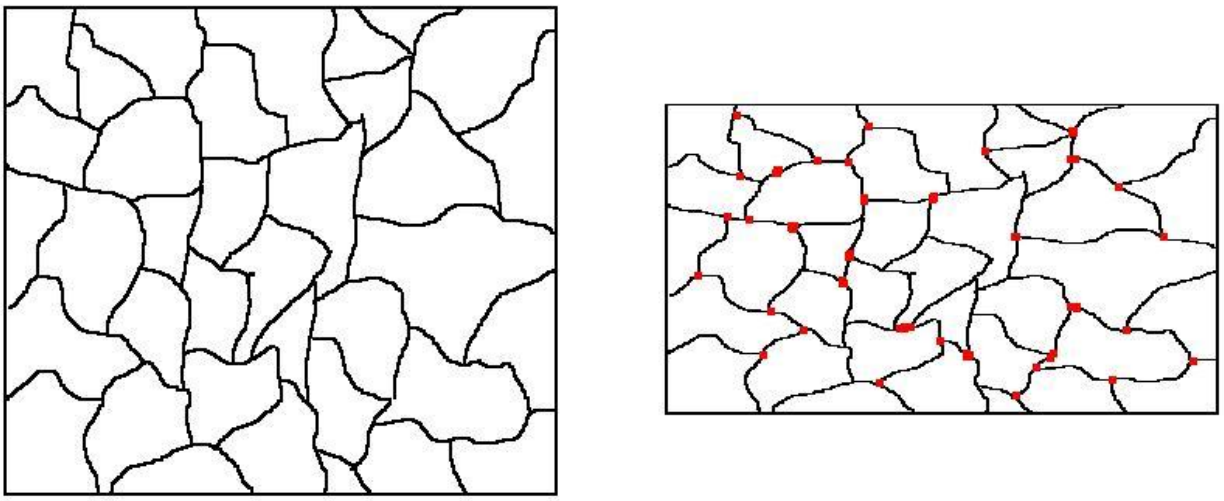

Figure 24: Cavities from during the forging process at the grain boundaries with high stress concentration, as marked by the red dots.

At higher temperatures, when the material is more malleable, the stress associated with forging can be more readily dispersed or absorbed through elastic deformation. The lower the temperature of the forging, the less malleable the material is, and the more likely it will form these cavities. Kinetically, cavities are ideal nucleation sites for solute dissolved in the matrix due to the ease of diffusion through free space. Carbides nucleate to these sites and affect the ductility as mentioned in section 2.6.3. The microstructural and mechanical results support the conclusion that increasing forging temperature decreases the concentration of carbides along the grain boundaries, and increases ductility of the material.

Sample A2 had a significant increase in carbide count, along with a decreased carbide size. It is likely that this sample was not recrystallized during solutionizing. Sample A2 was forged at the highest tested temperature, this causes the sample to also have the lowest internal strain. It was then solutionized at the lowest solutionizing temperature, giving the material the least energy input to resolve that strain and recrystallize. Forging condition A is associated with the highest temperature at which the grains will grow, and the microstructure suggests that the process of grain growth was not reached. During grain growth, the ϒ-grains would increase in size to reduce the surface area energy by coalescing. During this coalescing, carbides would have the opportunity to coalesce as well, increasing particle size, and decreasing the count.

During the mechanical testing of the samples, it was seen that forging temperature had the highest effect on ductility, and solutionizing had the highest effect on ultimate tensile strength. The relationship

between the forging temperature and ductility, as previously mentioned, is due to the decreased concentration of carbides along the grain boundaries. The relationship between the solutionizing temperature and the ultimate tensile strength is due to the size difference of the carbides and the ϒ-grains. The decreased size of both the carbides and the grains allowed for a higher degree of surface area contact between grains and carbides for the same volume. This interferes with dislocation movement in the samples, allowing for a higher ultimate tensile stress.

8 Conclusions

1) Increased forging temperature result in fewer carbides and higher ductility.
2) Decreasing solutionizing temperature increases carbide size, and increases yield strength.
3) Forging conditions A1, A2, and B1 will fail at an extension of greater than 40%.

9 Acknowledgements

I would not have been able to complete this project without the help of the following people. Professor Blair London, my advisor, has helped motivate me to put forward my best work, and was always there to tell me when I was straying from the right path. Robert Keener, of Carlton Forge Works, provided me with the topic of this project, was patient with me as I worked to complete this project in a form that was usable to his company. Creative Cutting, and Precision Machine, two machine shops in San Luis Obispo, kindly helped my extract usable samples from forged components of a material most machinists told me could not be machined. Robert Hayes of Metals Technology Inc. assisted me with some of the conceptual explanations of the data, as well as sample preparation. Megan Butala and Blake Reller, colleagues of mine, assisted me with the safe operation of the most complicated furnace I have ever used. I would like to extend my thanks to these people for their guidance and assistance over the year.

10 References

1) Carlton Forge Works. (2010). *Surefire Solutions (Brochure).*

2) Haynes International. (n.d.). *Haynes 230 Alloy Information.* Retrieved November 2011, from Haynes International: http://www.haynesintl.com/230HaynesAlloy.htm

3) Reed, R. C. (2006). *The Superalloys: Fundamentals and Applications.* Cambridge: Cambridge University Press.

4) Martinsson, Å. (2006). *Ageing Infl uence on Nickel-based Superalloys at Intermediate Temperatures.* Luleå University of Technology, Division of Engineering Materials.

5) Britannica. (n.d.). *Gas-Turbine Engine*. Retrieved February 2012, from Encyclopedia Britannica: http://www.britannica.com/EBchecked/topic/226481/gas-turbine-engine/45715/Gas-turbine-engine-cycles?anchor=ref134493

6) Lane, D. (2001). *The Brayton Cycle.* Retrieved February 2012, from University of Nevada Reno: http://web.me.unr.edu/me372/Spring2001/Brayton%20Cycle.pdf

7) SK Forging. (n.d.). *Ring Rolling*. Retrieved February 2012, from Forging Industry: http://www.forging-industry.com/bearing_manufacturer.asp?aid=17

8) ASM International. (2002). *Superalloys: A Technical Guide.* ASM International.

9) L. J. Chen, Y. H. (2000). High-Temperature Low-Cycle Fatigue Behavior of Haynes 230 Superalloy. *TMS: Superalloys* , pp. 573-581.

10) Bowman, R. (2000). Superalloys: A Primer and History. *9th International Symposium on Superalloys.* Champion, PA: TMS.

11) Moore, R. (1999). *Brayton Cycle Lecture Notes*. Retrieved February 2012, from Massachusetts Institute of Technology.

12) Baldan, A. (1992). Effects of Carbides and Cavitation on the Monkman-Grant Ductility of a Nickel-Based Superalloy. *Journal of Materials Science Letters* , 1315-1318.

13) H. Kaftelen, A. B. (2004). Comparative Creep Damage Assessments Using the Various Models. *Journal of Materials Science* , 4199-4210.

14) ABET Criteria for Accrediting Engineering Programs 2010-13, General Criteria for Baccalaureate Level Programs, General Criteria 3: Student Outcomes (c), www.abet.org/engineering-criteria-2012-2013.

15) Polsilapa. (2006). Reheat Treated Microstructures and Gamma Prime Particle Coarsening Behaviour at 900°C of Cast Nickel Based Superalloy IN-738. *Journal of Metals, Materials and Minerals*, 7-13.

16) Ruiz. (1998). Ductile Fracture of Thin Shells and Panels. Application to Containment Casings in Aeroengines. *Anales de Mecanica de la Fractura*, 34-48.